catalysts

MDPI

Article

Catalytic Activity Studies of Vanadia/Silica–Titania Catalysts in SVOC Partial Oxidation to Formaldehyde: Focus on the Catalyst Composition

Niina Koivikko [1,*], Tiina Laitinen [1], Anass Mouammine [1,2], Satu Ojala [1] and Riitta L. Keiski [1]

[1] Environmental and Chemical Engineering (ECE), Faculty of Technology, University of Oulu, P.O. Box 4300, FI-90014 Oulu, Finland; tiina.laitinen@oulu.fi (T.L.); mouammine@gmail.com (A.M.); satu.ojala@oulu.fi (S.O.); riitta.keiski@oulu.fi (R.L.K.)

[2] Laboratory of Catalysis and Corrosion of Materials (LCCM), Department of Chemistry, Faculty of Sciences, University of Chouaïb Doukkali, 20 Route de Ben Maachou, 24000 El Jadida, Morocco

* Correspondence: niina.koivikko@oulu.fi; Tel.: +358-(0)50-350-4188

Received: 31 December 2017; Accepted: 29 January 2018; Published: 2 February 2018

Abstract: In this work, silica–titania supported catalysts were prepared by a sol–gel method with various compositions. Vanadia was impregnated on SiO_2-TiO_2 with different loadings, and materials were investigated in the partial oxidation of methanol and methyl mercaptan to formaldehyde. The materials were characterized by using N_2 physisorption, X-ray diffraction (XRD), X-ray fluorescence spectroscopy (XRF), X-ray photoelectron spectroscopy (XPS), Scanning transmission electron microscope (STEM), NH_3-TPD, and Raman techniques. The activity results show the high importance of an optimized SiO_2-TiO_2 ratio to reach a high reactant conversion and formaldehyde yield. The characteristics of mixed oxides ensure a better dispersion of the active phase on the support and in this way increase the activity of the catalysts. The addition of vanadium pentoxide on the support lowered the optimal temperature of the reaction significantly. Increasing the vanadia loading from 1.5% to 2.5% did not result in higher formaldehyde concentration. Over the 1.5%V_2O_5/SiO_2 + 30%TiO_2 catalyst, the optimal selectivity was reached at 415 °C when the maximum formaldehyde concentration was ~1000 ppm.

Keywords: vanadium pentoxide; titanium dioxide; silicon dioxide; utilization of VOC; oxidative dehydrogenation; oxidative desulfurization

1. Introduction

Silicon dioxide SiO_2 and titanium dioxide TiO_2 support materials are used extensively in academic research and in industrial applications. Mixed SiO_2-TiO_2 materials have attracted many researchers, because it has been shown that mixed SiO_2-TiO_2 materials can provide certain advantages over single oxides. Benefits such as stronger metal–support interactions, higher acidity compared to single oxides, better resistance to sintering, and resistance against sulfur poisoning have been observed in earlier studies [1–7].

The sol–gel preparation procedure, not only being a rather easy way to prepare catalyst materials, provides advantages over the SiO_2-TiO_2 preparation process [6,8,9]. The sol–gel preparation steps include sol (colloid suspension) preparation, alkoxysilane hydrolysis, and condensation of silica and titania precursors. This leads to a structure where Ti is homogeneously dispersed in the silica matrix, which often results in better activity in oxidation applications. The presence of only a small amount of Ti leads to structural changes of the support as it causes narrowing of the Si-O bond length distribution. The support has a disordered tetrahedral structure in which Ti atoms are incorporated into the silica network [5]. Due to the advantages of silica–titania supports, they are used as supports for vanadia-containing catalysts in different applications [10–18].

This work focuses on the utilization of sulfur-containing volatile organic compound (SVOC) emissions. These emissions raise a lot of discussion, especially in the pulp and paper industry, as they are very odorous at low concentrations and their emission levels typically vary. Nowadays, methanol-containing streams are collected from the process and used as an energy source [19]. To increase the fuel value of methanol, the streams are concentrated and then directed to the combustion. Since the streams are utilized in the pulping process as an energy source, the formation of carbon dioxide emissions cannot be avoided. New approaches are needed to minimize the environmental load originating from methanol emissions and to utilize the stream in the production of new valuable chemicals more efficiently.

Compounds such as methyl mercaptan (MM), dimethyl sulphide (DMS), dimethyl disulphide (DMDS) and sulfur dioxide (SO_2) are present in mostly methanol (MeOH) and water containing stripper overhead gases (SOG) of the pulp mills [19,20]. In this approach, the MM containing methanol is considered as the raw material for formaldehyde production. We have previously shown the good activity of V_2O_5/SiO_2-TiO_2 in this application [21], and thus the aims of the current study lie in optimizing the catalyst composition and in finding more information from the catalyst properties affecting the formation of formaldehyde and possible other products.

Methanol oxidative dehydrogenation to formaldehyde over different vanadia catalysts has been under intensive investigation during recent decades [15,22–29]; however, the utilization of the contaminated methanol by sulfur compounds, such as methyl mercaptan, has been less studied. It has been stated that the performance of the materials depends on the surface structure of the vanadium on the chosen support. According to current knowledge, the activity of the vanadium catalysts is largely due to the presence of VO_4 sites on the supporting materials [30].

2. Results and Discussion

2.1. Characterization of Catalysts

Specific surface areas, pore volumes, and pore sizes of all fresh supports and catalysts are given in Table 1 with the catalyst elemental analysis results measured by X-ray fluorescence spectroscopy (XRF). In addition, the vanadia surface loadings are given for the catalysts.

Table 1. The Brunauer-Emmett–Teller Barret-Joyner-Halenda (BET-BJH) method and X-ray fluorescence spectroscopy (XRF) results calculated as oxides for the supports and vanadium-containing catalysts.

Support	Surface Area	Total Pore Volume	Pore Size	XRF [%]			Surface Loading
	[$m^2 g^{-1}$]	[$cm^3 g^{-1}$]	[nm]	V_2O_5	SiO_2	TiO_2	V_{atom} nm^{-2}
Si	225	0.1	1.9	-	~100	-	-
Ti	10	0.02	6.8	-	-	~100	-
SiTi(10)	560	0.28	2.0	-	70	9	-
SiTi(30)	590	0.35	2.3	-	57	27	-
SiTi(60)	220	0.11	2.1	-	35	56	-
Catalyst							
1.5V/Si	140	0.06	1.9	1.56	98	-	0.74
1.5V/Ti	10	0.01	7.3	1.44	-	98	9.54
0.75V/SiTi(30)	560	0.33	2.3	0.65	58	27	0.08
1.5V/SiTi(30)	500	0.3	2.3	1.7	66	31	0.23
2.5V/SiTi(30)	470	0.28	2.3	2.4	66	31	0.34

Pure silica (denoted as Si) has a much higher surface area and pore volume compared to pure TiO_2 (denoted as Ti), 225 m^2 g^{-1} and 11 m^2 g^{-1}, respectively. Addition of titanium into silica leads to higher surface areas even with such low titania loadings as 10%. While titanium dioxide as a single oxide has a low surface area, the mixed metal oxide SiO_2-TiO_2 (SiTi) with the Si:Ti ratios of 90:10 and 70:30 shows notably higher surface area, for example over 550 m^2 g^{-1}. For SiTi(60) the surface area was ~220 m^2 g^{-1} as a results of the higher Ti-content in the support. Generally, the surface areas of vanadia-containing catalysts were lower than surface areas of the corresponding supports due to

partial blockage of the pores of the support by vanadia particles. This has also been observed by other researchers [7]. Pore sizes are on the level of ~2 nm for all silica containing catalysts. Titania supported catalysts have pore sizes between 6.8 nm and 7.3 nm. Based on the XRF results, the desired amount of V_2O_5 as well as the SiO_2-TiO_2 ratio were obtained by the sol–gel procedure rather well.

The X-ray diffraction (XRD) patterns of pure Ti, SiTi(10), SiTi(30) and 2.5%V/SiTi(30) (calcination at 500 °C) are shown in Figure 1. The increase in Ti concentration in the mixed SiTi catalysts results in an increase in the peak intensity in the XRD diffractogram. As silica is amorphous, the changes in the spectra are related to the amount of crystalline titania which are shown by more intense XRD peaks. Titania is mainly in the anatase form (an intense peak at 2θ = 25.28) with a crystallite size of approximately 20 nm in a pure TiO_2 sample. The crystallite size of anatase in SiTi(30) and 2.5%V/SiTi(30) was ~7 nm. The pure TiO_2 sample also showed the presence of small amounts of rutile-phase (7%), which was not visible in the mixed oxides. The XRD results did not show the peak corresponding to V_2O_5 (2θ = 20.26) with the V_2O_5-loading of 2.5%. This may be due to low vanadia loading, but it indicates also that vanadium oxide is probably present in a well-dispersed state on the SiTi(30) support. To be able to detect V_2O_5, for example, on the anatase form of titania, earlier studies have reported that the amount of vanadia should be over 5% or even higher [7,31].

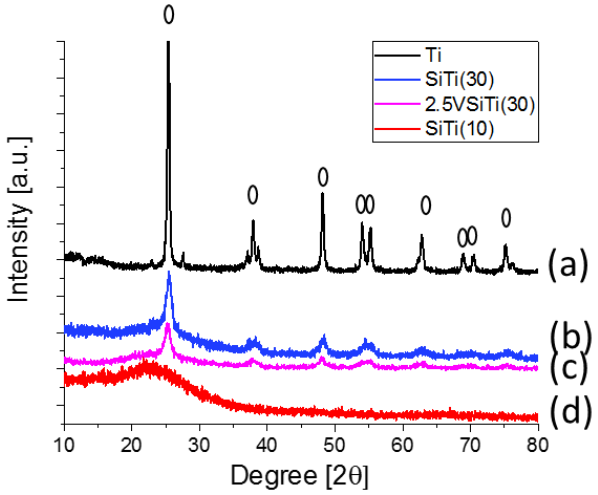

Figure 1. XRD patterns of the SiO_2-TiO_2 catalyst with different ratios of silica and titania (calcined at 500 °C): (**a**) Ti; (**b**) SiTi(30); (**c**) 2.5V/SiTi(30); (**d**) SiTi(10).

The X-ray photoelectron spectroscopy (XPS) analysis was done mainly to find out the oxidation degree of vanadium. Table 2 presents the binding energy (BE) values of V 2p, O 1s, Si 2p and Ti 2p for the fresh 1.5V/Si, 1.5V/Ti and 1.5V/SiTi(30). The charge correction was made by adjusting the main C 1s peak at 284.8 eV [32].

Table 2. Binding energies and full width at the half-maximum (FWHM) values presented in the brackets for the fresh 1.5%V_2O_5 catalysts supported on SiO_2, TiO_2 and SiTi(30).

Catalyst	V 2p [eV]		O 1s [eV]		Si 2p [eV]	Ti 2p [eV]	
	V $2p_{3/2}$	V $2p_{1/2}$				Ti $2p_{1/2}$	Ti $2p_{3/2}$
1.5V/Si	517.49 (1.86)	524.85 (3.37)	533.17 (1.78)	530.46 (1.58)	103.86 (1.66)	- -	- -
1.5V/Ti	517.62 (1.58)	524.94 (3.37)	531.92 (1.64)	530.41 (1.29)	- -	464.84 (2.13)	459.19 (1.27)
1.5V/SiTi(30)	517.64 (2.67)	525.06 (3.37)	532.88 (1.86)	530.43 (1.40)	103.60 (1.65)	465.00 (2.27)	459.20 (2.02)

The binding energy of the V $2p_{3/2}$ core level depends on the oxidation state of the V cation; the curve fitting of V $2p_{3/2}$ is often used to detect the different vanadium cation oxidation states present in vanadium oxide samples [32,33]. In this work, to define the oxidation states of vanadium, the data was collected together for V 2p and O 1s. The results are presented in Figure 2. For the V 2p, the spectra show a typical two-peak structure (V $2p_{3/2}$ and V $2p_{1/2}$) [33,34]. For each of the three catalysts the V $2p_{3/2}$ spectra showed a peak at a binding energy value of ~517 eV (517.49–517.64 eV), indicating the oxidation state of V^{5+}. For the V $2p_{1/2}$, spectra showed a peak at BE values between 524.8–525.0 eV, which also is connected to oxidation state V^{5+}. It was expected based on the literature that the vanadium could be present on the catalyst surface as V_2O_5 or a lower-valence vanadium oxide [32]. The typical value for full width at half-maximum (FWHM) for pure V_2O_5 is rather small (on the level of less than 2 eV). In our case this is consistent for Si and Ti supported vanadia. In the case of SiTi(30) support, the value is somewhat higher, indicating the possibility of the presence of other oxidation states of vanadium. The large widths of the V 2p lines might be also due to defects at the surface and/or disproportion at the surface [35].

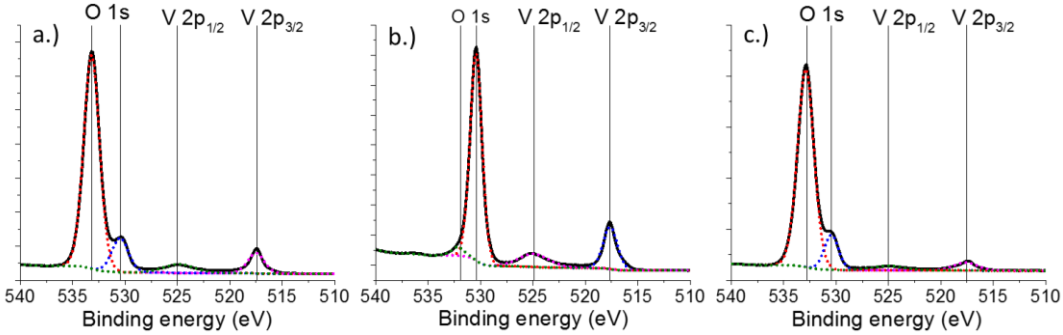

Figure 2. Electron spectra of (**a**) 1.5V/Si; (**b**) 1.5V/Ti; (**c**) 1.5V/SiTi(30) (calcined at 500 °C) studied with XPS.

The O 1s signal showed two clear peaks for silica containing samples: a major one at ca 532.9 eV (Si-O in the SiO_2 lattice) and a minor one at ca 530.3 eV (vanadium bonded oxygen) [12]. In addition, for the Si-containing samples the deconvolution of the Si 2p spectra revealed one peak at the binding energy values between 103.60–103.86 eV (see Table 2). Stakheev et al. [2] have observed earlier the presence of Si 2p peaks between 102.5–104.1 eV; that position depends on the added Ti amount in the sample.

The binding energy values for Ti $2p_{3/2}$ remain approximately the same for both Ti-containing samples (~459.20 eV; see the Table 2). The addition of Ti to Si leads to a shift in the Si $2p_{1/2}$ peak to a lower binding energy (total shift 0.26 eV). For the V/Ti catalyst the O 1s spectrum shows a peak centered at 530.41 eV and a tail extending to higher binding energy (centered at 531.92 eV). Odriozola et al. [36] explained that for the O 1s peak at ca. 532 eV, a so-called tail can be resolved and explained by the presence of hydroxyl species. Keränen et al. in 2003 [18] have also reported O 1s values of 530.0 and 531.6 eV for the V/Ti catalyst, which similarly explains the difference between the two peaks. For the SiTi support, in addition to the band maxima of O 1s observed at 532.88 eV (Si-O-Si) another band was observed at 530.43 eV, which is explained by either oxygen in Si-O-Ti structure or vanadium bonded oxygen [37]. Furthermore, the surface ratio of Si and Ti determined for 1.5%V/SiTi(30) was 80:20, which is very close to that determined by XRF for the bulk structure of the support. This gives an indication of the homogeneity of the prepared support.

The total acidities of SiTi materials with different ratios were determined with NH_3-TPD. The total amount of the desorbed ammonia representing the total amount of acid sites can be seen from Figure 3 (determined between 50 °C and 500 °C). Itoh et al. [1] have noted in 1974 that the acidity follows the trend of the surface area, but also that the total acidity is increased when SiO_2 is added to TiO_2. This is

also expected based on the point of zero charge (PZC) values of the two oxides (pH at PZC for TiO_2 and SiO_2 are 6.0–6.4 and 2–4, respectively) [30]. In the same way, the current work shows that pure Ti has low acidity, which is increased after addition of silica ending up to pure SiO_2 that has the highest total acidity of the tested materials. The trend of total acidity based on NH_3-TPD is Si > SiTi(10) > SiTi(30) > SiTi(60) > Ti. Stakheev et al. in 1993 and Kobayashi et al. in 2005 [2,7] have presented results where the highest acidity was gained with the Si:Ti molar ratio of 1:1 determined by a titration method. This was not observed in our case. Considering the surface area of the samples, we did not notice clear correlation with the total acidity and the specific surface area of the samples, as shown in Figure 3. Concerning the strength of the acid sites, all the catalysts showed a broad low-temperature desorption peak (see Figure 4) centered at about 100 °C, which indicates the existence of mostly weak acid sites.

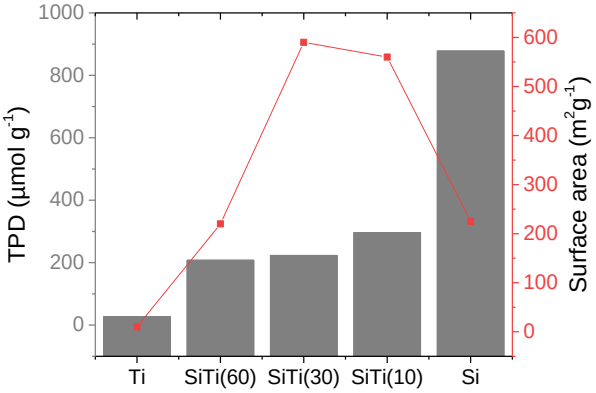

Figure 3. The results of the acidity of the silica and/or titania support materials measured with NH_3-TPD.

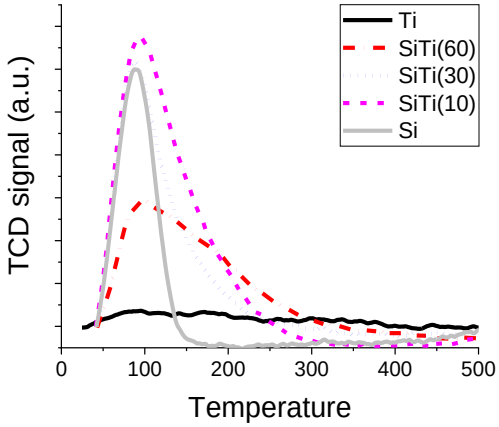

Figure 4. TPD profiles for ammonia desorption for silica and/or titania containing supports.

The STEM (Scanning transmission electron microscope) images of fresh catalysts, 1.5V/Si, 1.5V/Ti and 1.5V/SiTi(30), are presented in Figure 5. The STEM analysis was performed to investigate the microstructure of the catalysts. The EDS (Energy dispersive X-ray spectroscopy) mapping revealed the dispersions of vanadium on the catalysts' surface. On the silica support, vanadia forms bigger clusters (~250 nm) (see Figure 5a). This is due to the rather inert silica surface [38]. In the case of titanium dioxide and especially in the support of mixed SiTi, the particle size was much smaller and vanadium was better dispersed. Basic oxides usually exhibit good dispersion of vanadia and for that reason addition of less acidic titania to silica may result in better dispersion [39,40]. In the case of Ti support, the V_2O_5 is unevenly dispersed on the surface (see Figure 5b). The surface loading of V on TiO_2 is much higher (9.54 V_{atom} nm^{-2}) compared to the other catalysts, which have the surface

loadings on the level of 0.08–0.74 V_{atom} nm^{-2}. This explains why vanadia is not well-dispersed on pure TiO_2 support.

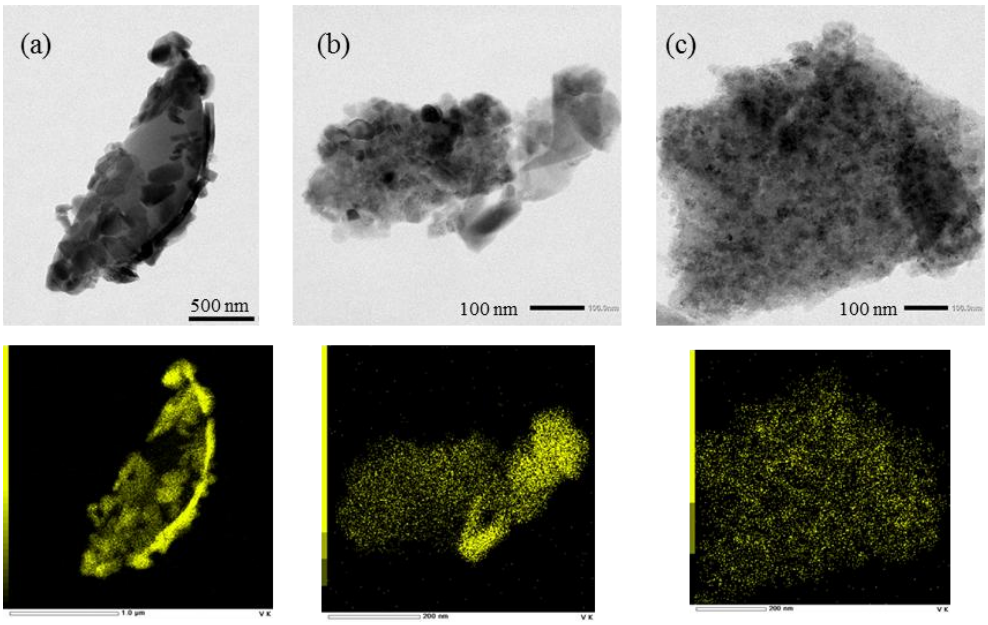

Figure 5. Scanning transmission electron microscope (STEM) images and Energy dispersive X-ray spectroscopy (EDS) mapping results of vanadia for fresh (**a**) 1.5V/Si (**b**) 1.5V/Ti (**c**) 1.5V/SiTi(30).

2.2. Results of Catalytic Oxidation Tests

The first series of the prepared catalysts and performance of the catalysts in the oxidation reaction of methanol (MeOH) and methyl mercaptan (MM) are presented in Figure 6a,b. In Figure 6a, the activity of the supports Si, Ti, and SiTi(30) are shown; and in Figure 6b, the effect of SiTi ratio on the gained formaldehyde concentration is presented. The earlier research results [21] show remarkably better activity of the support material in the oxidation of MeOH and MM as a mixture when Ti is added to Si. In this study, the main focus was on the investigation of the changes in activity to form formaldehyde with different Si:Ti ratios.

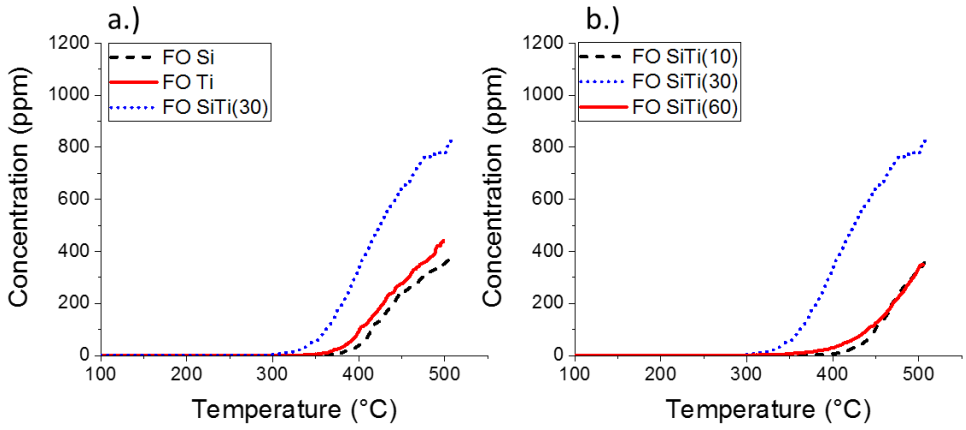

Figure 6. Formation of formaldehyde over (**a**) Si, Ti and SiTi(30) and (**b**) SiTi(10), SiTi(30) and SiTi(60) during the oxidation of methanol and methyl mercaptan (feed 500 ppm + 500 ppm, heating rate 5 °C min^{-1}).

As expected, with the addition of 30% titania to silica the formaldehyde production rose to more than double, compared to single oxide supports. What was unexpected (see Figure 6b) was that the SiTi ratio was crucial in gaining the highest formaldehyde concentration values. With the addition of 10% titania, no signs of activity improvement were observed. The 60% titania addition resulted only in ~400 ppm formaldehyde concentration, which is the same as with 10% Ti. Based on these results, it was decided to continue the activity testing with the SiTi(30) support as it was clearly the most active one from the tested materials with over 800 ppm formaldehyde production at 500 °C.

The addition of vanadia on the support was the second step in the current work. The 1.5% vanadium pentoxide addition increased the activity of all the tested catalysts. Results of the 1.5%V catalysts are presented in Figure 7. With single oxide silica and titania supports, the formaldehyde concentration rose to 1000 ppm, which was over 500 ppm more than with single oxide supports before vanadia addition. The addition of vanadia on SiTi(30) lowers the optimal reaction temperature significantly. For 1.5V/SiTi(30), the optimal temperature was already reached at around 400 °C.

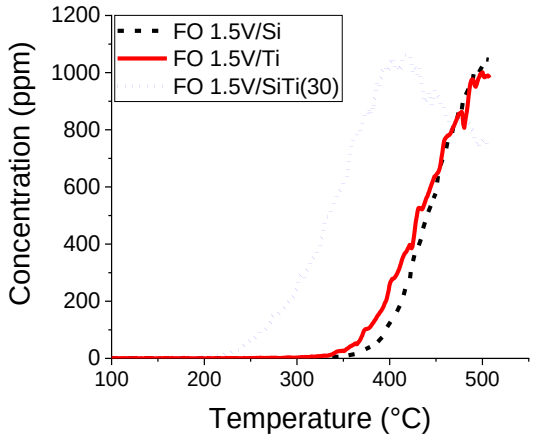

Figure 7. Formation of formaldehyde over pure silica or/and titania supports with 1.5% vanadium pentoxide during the oxidation of methanol and methyl mercaptan (feed 500 ppm + 500 ppm, heating rate 5 °C min^{-1}).

The results indicate that the good performance of single oxide Si or Ti supported catalysts requires an oxidation temperature over 500 °C—which we did not test—since lower temperatures are more interesting from an energy point of view, and because vanadium pentoxide as the catalyst material sets some limits to the activity testing. The melting point of V_2O_5 is 690 °C [41], and we wanted to stay at lower temperatures to minimize the sintering of vanadia during the reaction. Vanadium pentoxide as an active compound for MeOH and MM oxidation has been tested also at temperatures over 500 °C by Laitinen et al., 2016 [42].

As mentioned, both the Si:Ti ratio and the active compound V_2O_5 have a significant role in the reaction in reaching maximum formaldehyde production. The most active catalyst, 1.5V/SiTi(30), has the highest surface area and the best dispersion of vanadia based on the characterization. It has been shown that the dispersion of the active phase is dependent on the support composition. However, the results do not fully support the significance of the surface area, since SiTi(10) has higher specific surface area compared to single oxide silica, but it does not positively influence the activity results. On the other hand, the STEM results showed that the dispersion of the active phase is much better with the SiTi(30) support. Vanadia dispersion surely has a role in the activity of the material, but more testing with each of the materials with different vanadia particle sizes should be done. The effect of the total acidity in the activity is controversial. It is shown in the work of other researchers [1,7] that formaldehyde can be produced only with acidic oxides. However, the current results do not fully support these findings as pure silica resulted in the highest acidity of the tested materials, yet the

lowest formaldehyde production. It seems that the acidity has to be at certain optimal level—not too high and not too low. In addition, the quality of acid sites (Brønsted-Lewis) may play a role, however we were not able to qualify the sites in the current study. Based on Tanabe et al. [43], SiO_2 contains mainly Brønsted acid sites (BAS) and TiO_2 Lewis acid sites (LAS). In the mixed oxide when TiO_2 is added to SiO_2, the amount of BAS in the material should increase. If this is true, the existence of both acid sites is important to be able to carry out the reactions under investigation. In addition, it has been also examined that the V/Ti catalysts show the presence of both BAS and LAS. The BAS are dominating acid sites in V_2O_2 [3]. The addition of vanadia to silica–titania support increases further the amount of BAS in the sample [44].

One of the objectives of this research was also to study the effect of the amount of vanadia impregnated on the catalysts. The results of SiTi(30) supported vanadia catalysts with different vanadia loadings (0.75%, 1.5% and 2.5%) are presented in Figure 8. As noted earlier, the addition of vanadia lowers the optimal temperature and the temperature where the reactions start. These current results reveal that the addition of vanadia from 1.5% to 2.5% does not result in increasing activity of the catalyst. Based on this finding we can expect that increasing the vanadia amount is not significant and it is reasonable to use a low amount of vanadia. This result is supported by Mouammine et al. [45], as in the case of V/Ti the increase in the V amount from 1.5% to 3% and to 10% did not result in higher formaldehyde yields.

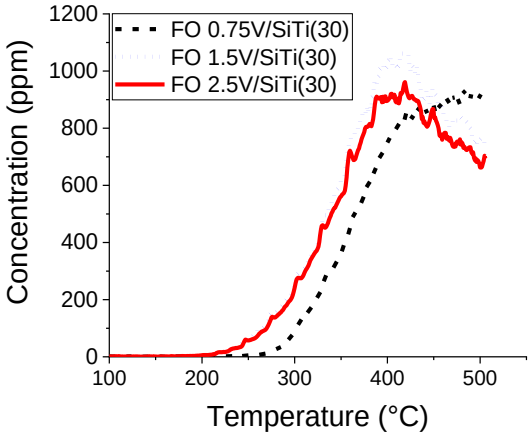

Figure 8. Formation of formaldehyde over silica–titania (V/SiTi(30)) catalysts with different V amounts (feed 500 ppm MeOH + 500 ppm MM, heating rate of 5 °C min^{-1}).

The main results from all the activity experiments are presented in Table 3. The table is presenting the key temperatures for each catalyst; the temperature in which the formation of the formaldehyde begins (A) and the temperature when the formaldehyde concentration reaches the maximum value during the experiment (B). From these values, it can be seen, that the formation of formaldehyde begins at the temperature level between 210 °C and 410 °C. The 1.5V/SiTi(30) catalyst has an optimal temperature of 415 °C (1060 ppm) and at 500 °C the formaldehyde concentration is only 760 ppm. This means that, after the optimal temperature, formaldehyde has reacted further to CO.

Table 3. Comparison of different catalysts in the reaction (key temperatures and gained maximum formaldehyde concentrations). Feed: 500 ppm methanol and 500 ppm methyl mercaptan, reaction temperature from room temperature to 500 °C.

Catalyst	Temperature A *	Temperature B #	Formaldehyde Concentration at Temp. B	Formaldehyde Concentration at 500 °C
	[°C]	[°C]	[ppm]	[ppm]
SiO_2	380	500	360	360
TiO_2	360	500	440	440
SiTi(10)	410	500	330	330
SiTi(30)	315	500	780	780
SiTi(60)	365	500	340	340
0.75%V/SiTi(30)	215	480	930	918
1.5%V/SiTi(30)	215	415	1060	760
1.5%VSi	350	500	1030	1030
1.5%VTi	335	500	1000	1000
2.5%V/SiTi(30)	215	420	960	660

* The temperature when the formation of formaldehyde begins (over 10 ppm) during the activity test. # The temperature when the formaldehyde concentration is highest during the test (optimal temperature for specific catalyst).

All the activity tests were repeated with the same catalyst twice. In Figure 9, the results of the repeated tests for 0.75V/SiTi(30), 1.5V/SiTi(30), and 2.5V/SiTi(30) are presented. The activity of the catalyst and the formation of formaldehyde follow exactly the same route in each test showing good repeatability of the test, but also giving some indications on the stability of the catalyst.

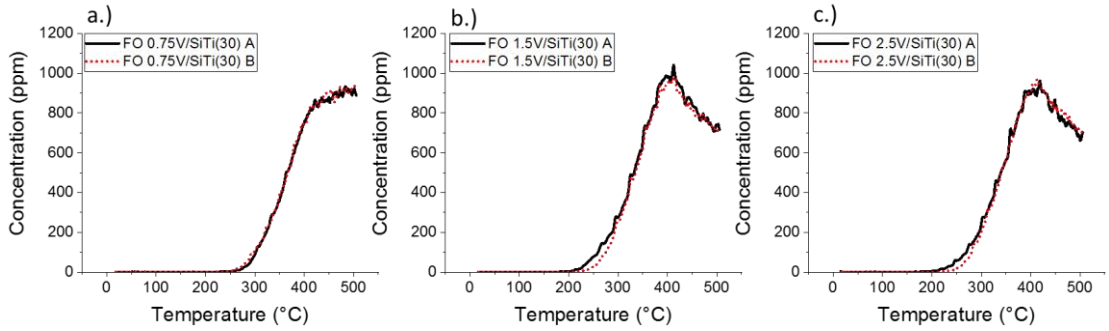

Figure 9. Formation of formaldehyde of the repeated tests for (**a**) 0.75V/SiTi(30); (**b**) 1.5V/SiTi(30) and (**c**) 2.5V/SiTi(30) (feed 500 ppm MeOH + 500 ppm MM, heating rate of 5 °C min^{-1}, A referring to test 1 and B referring to the repeated test 2).

In addition, more information on the stability of the 1.5%V catalyst with Si, Ti, and SiTi(30) supports was also revealed during the test at the optimal temperature for 8 h. The formaldehyde concentration remained unchanged through the whole experiment and no signs of activity loss were observed (figures not shown here).

Molecular structures of the dispersed vanadium oxide species on the support can be determined with Raman spectroscopy. The surface analysis was performed in order to investigate the structures of the fresh materials and if any changes after the 8 h stability test could be detected. The measurements were performed with Timegated® Raman device, in which the effect of the fluorescence is reduced from the resulting spectra. Figure 10 presents the Raman spectra of Si-, Ti-, SiTi(30)-supported V_2O_5 and bulk V_2O_5.

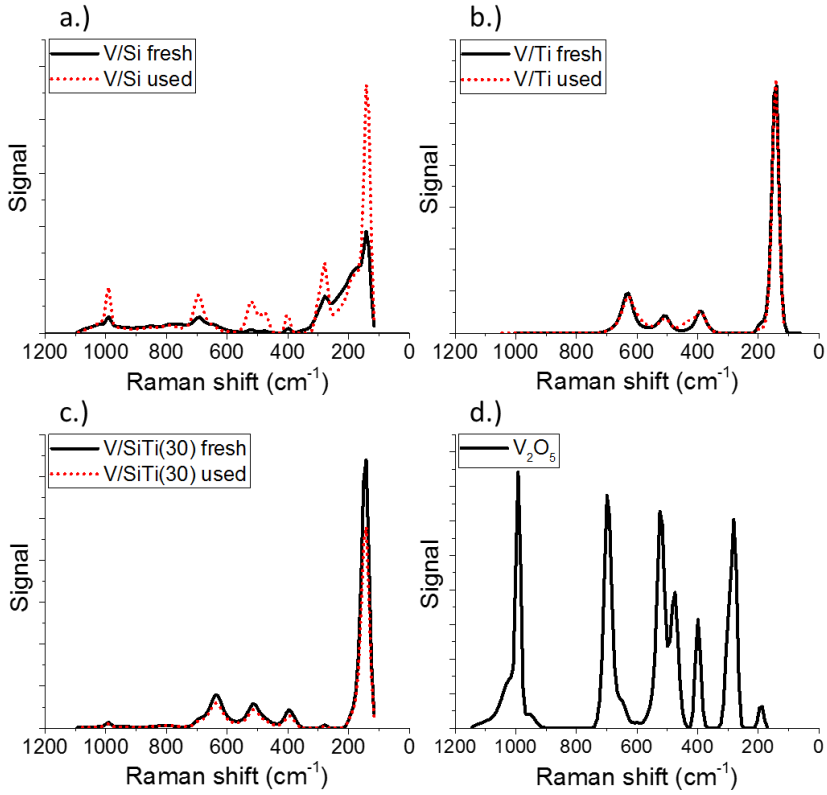

Figure 10. Timegated Raman spectra of (**a**) 1.5V/Si, (**b**) 1.5V/Ti, (**c**) 1.5V/SiTi(30) and (**d**) bulk V_2O_5.

Bulk vanadium pentoxide gives peaks at ~144, 188, 280, 398, 474, 524, 697, 940, 992 and 1030 cm^{-1}. The peak at 992 cm^{-1} is related to the symmetric stretching of V=O groups in the bulk vanadia [18,46] assigned as crystalline V_2O_5. It has been proposed that the less intense peaks at 940 cm^{-1} and 1030 cm^{-1} originate from isolated and polymerized surface vanadia species, respectively [10,47,48]. The intense peak at 700 cm^{-1} corresponds to lattice vibrations localized within the V-O-V bridge in the V_2O_5 structure.

For the Si-supported V_2O_5, similar features to crystalline V_2O_5 exist, since the observed peaks are in line with the peak positions of the bulk V_2O_5. For Ti-supported V_2O_5, the intense peaks from the TiO_2-support are visible at 142, 391, 510 and 633 cm^{-1} corresponding to the anatase TiO_2 [18]. In the case of both vanadia- and titania-containing samples the definite identification of the Raman spectra is difficult due to the proximity of intense crystalline V_2O_5 (~144 cm^{-1}) and TiO_2 anatase (~147 cm^{-1}) peaks. There were no peaks visible at 800–1000 cm^{-1}, which would be an indication that the dispersion of the isolated VO_x species on V/Ti was better than with V/Si. For the SiTi(30)-supported V_2O_5, the VO_x species at 278 and 991 cm^{-1} seem to be visible. Compared to the single oxide Ti support, a small peak at 991 cm^{-1} (V_2O_5) exists in the spectrum SiTi(30).

When the Raman spectra of the fresh catalysts and the catalysts after 8 h of testing were compared, no significant differences between the fresh and used samples were observed. The visible changes are only due to the changes in the signal intensity, which may in this case indicate more crystalline material (such as in the case of used VSi). This gives an indication on the stability of the material in presence of sulfur. More studies will be done in the future to find out details related to the oxidation of methanol in the presence of sulfur-containing compounds.

Figure 11 presents the formation of by-products over the 1.5V/SiTi(30) catalyst to study the performance of the catalyst in more detail. The main products were sulfur dioxide, carbon monoxide, and dimethyl disulphide, as expected based on the literature [19,49].

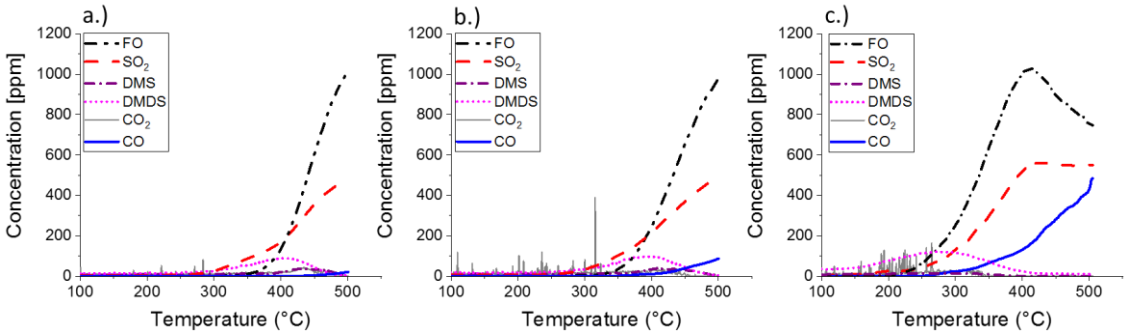

Figure 11. Formation of by-products in the oxidation of the mixture of methanol and methyl mercaptan (500 ppm + 500 ppm) over (**a**) 1.5V/Si; (**b**) 1.5V/Ti and (**c**) 1.5V/SiTi(30) catalysts (feed 500 ppm + 500 ppm, heating rate of 5 °C min^{-1}).

The formation of the products are results of the following reactions:

$$CH_3OH + 1/2O_2 \rightarrow CH_2O + H_2O \quad (1)$$

$$CH_3SH + 2O_2 \rightarrow CH_2O + SO_2 + H_2O \quad (2)$$

$$CH_3OH + 3/2O_2 \rightarrow CO_2 + 2H_2O \quad (3)$$

$$2CH_3SH + 1/2O_2 \rightarrow CH_3SSCH_3 + H_2O \quad (4)$$

$$CH_2O + 1/2O_2 \rightarrow CO + H_2O \quad (5)$$

$$CH_2O + O_2 \rightarrow CO_2 + H_2O \quad (6)$$

In the oxidation reaction of MM, sulfur dioxide is formed according to Reaction (2) and is the main product of the reaction together with formaldehyde. As formaldehyde reaches ~1000 ppm concentration in each of the tests, the formed SO_2 concentration is about 550 ppm in each presented case. The other reaction products, CO_2, H_2O and DMDS, are formed according to Reactions (3) and (4), which are complete oxidation of methanol and partial oxidation of MM to DMDS. The formation of DMDS is observed in the temperature range of 300 °C–450 °C for 1.5V/Si and 1.5V/Ti, reaching the maximum value approximately at 400 °C. For the SiTi supported catalyst the max. DMDS concentration of ~120 ppm is reached at temperature below 300 °C. The formation of carbon monoxide is detected when formaldehyde reacts further (Reactions (5) and (6)). This is clearly visible in the case of V/SiTi(30) at around 400 °C when the formaldehyde concentration starts to decrease and a significant amount of CO is formed. In other cases, the CO concentration stays at rather low levels (max. 85 ppm at 500 °C) as the concentration of formaldehyde is not decreasing during the temperature range used in the tests.

To compare the performance of the support and the vanadium containing catalyst, the concentrations of each gaseous product compound are presented in Figure 12. The comparison shown in the figure is done between the SiTi(30) support, marked as 1, and the 1.5V/SiTi(30) catalyst, marked as 2. To start with the reactants, there is a significant difference in the reaction when comparing the support and the catalyst. After vanadia addition on the support, the activity of the material in the reaction becomes significantly higher, which is visible in the changes in the reaction of MM. After vanadia addition, MM is already consumed starting at temperatures below 200 °C. Over the support, MM consumption begins at temperatures above 250 °C. MM conversion reached ~100% in all the tests. During the catalytic tests, the consumption of methanol begins at temperatures of around 300 °C. The differences in methanol partial oxidation activities between the support and the catalyst are not that significant, but the rate of the reaction is faster and higher methanol conversion is reached over the vanadia containing catalyst.

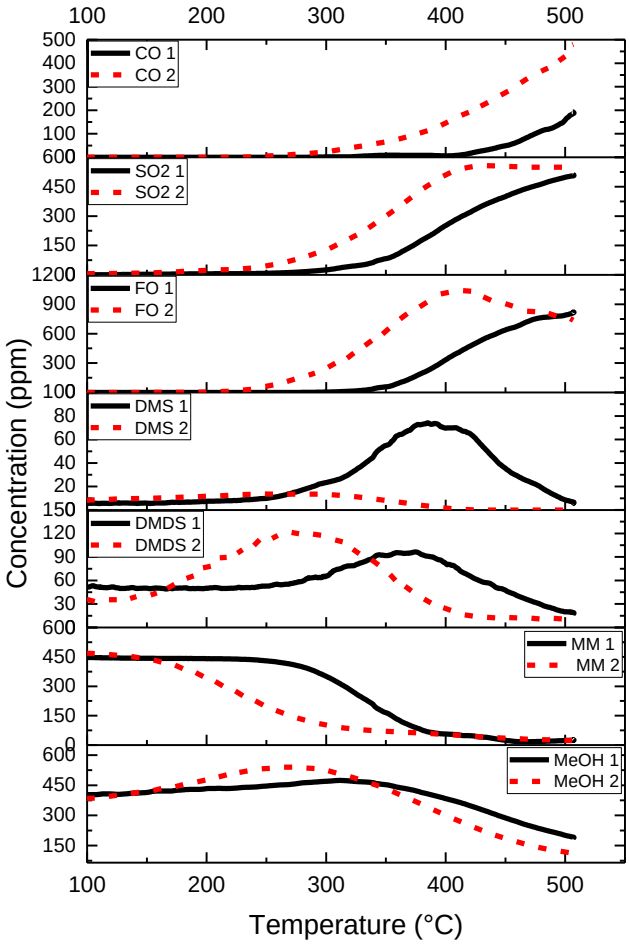

Figure 12. Formation of by-products in the oxidation of the mixture of methanol and methyl mercaptan (500 ppm + 500 ppm) over the SiTi(30) support(1) and 1.5V/SiTi(30) catalyst(2) (feed 500 ppm + 500 ppm, heating rate of 5 °C min^{-1}).

As explained earlier, the addition of vanadia on the SiTi support lowers the optimal temperature significantly, after which the formaldehyde concentration decreases when it starts to react further in the used reaction conditions. Figure 12 shows clearly the difference between the support and the catalyst in terms of the CO concentration, as in the presence of the VSiTi catalyst the CO concentration is more than twice the concentration reached over the SiTi support material. DMS concentration in both the experiments stays under 80 ppm, and for V/SiTi(30) the formation is insignificant. DMDS, for both the support and the vanadia containing catalyst, is observed as an intermediate product between 300–450 °C and 200–350 °C, respectively.

3. Materials and Methods

In this research, 5 different supports were prepared: pure SiO_2, TiO_2, and SiO_2-TiO_2 supports with the Si:Ti ratios of 90:10, 70:30, and 40:60 with no specific structure in target. After the optimization of the support composition, different amounts of vanadium pentoxide, 0.75%, 1.5%, and 2.5%, were impregnated on the support.

Mesoporous silica was prepared using the sol–gel method. A mass of 34.74 g of tetraethoxy orthosilicate ($Si(OC_2H_5)_4$, TEOS, 98% Sigma-Aldrich, St. Louis, MO, USA) was added to 54 g of absolute ethanol (Merck, Darmstadt, Germany) with a molar ratio of 1:7. A few drops of nitric acid were added to the solution to catalyze the hydrolysis step of the preparation. After dissolution of the silicon precursor, 24.5 g of ultrapure water (Sigma Aldrich, St. Louis, MO, USA), with a molar ratio

of 1:8, was added dropwise. The obtained sol was then left for 15 days for aging. The TiO_2-support was synthesized using the sol–gel method. A Ti-containing solution was prepared first by adding 43 g titanium butoxide ($Ti(OBu)_4$, TBOT, 97% Sigma-Aldrich, St. Louis, MO, USA) to 83 g absolute ethanol with a molar ratio of 1:14 and stirred until complete dissolution of the Ti precursor. Then, ultra-pure water was added drop by drop until a molar ratio of 1:15 was reached.

The titania doped silica supports were prepared by dissolving an appropriate amount of both titanium and silicon precursors in absolute ethanol (molar ratio 1:14) to obtain a composition of SiO_2(1-x)TiO_2(x) (with x = 0.1; 0.3; 0.6). A few drops of nitric acid were added to the solution, and then ultra-pure water was added with a molar ratio of 1:15. The solution was kept under stirring for 2 h. The final support was obtained after drying the gel at 90 °C overnight, and the dried gel was calcined at 500 °C for 2 h.

Addition of the active phase was done by using a wet impregnation method. At room temperature the appropriate amount of the vanadium precursor, vanadyl acetylacetonate ($VO(acac)_2$, 98% Sigma-Alrich, St. Louis, MO, USA) was dissolved in methanol. The support was added to the solution and kept under mechanical stirring overnight. The final catalysts were obtained after drying on a sand bath at 80 °C, and calcining at 500 °C for 2 h. The target amounts of vanadium pentoxide V_2O_5 on the support were 0.75 wt %, 1.5 wt %, and 2.5 wt %.

The materials prepared for this study and the abbreviations used in this article are presented in Table 4.

Table 4. Catalysts prepared for the oxidation studies.

Support/Catalyst	Abbreviation
SiO_2	Si
TiO_2	Ti
SiO_2 + 10%TiO_2	SiTi(10)
SiO_2 + 30%TiO_2	SiTi(30)
SiO_2 + 60%TiO_2	SiTi(60)
0.75%V_2O_5/ SiO_2+30%TiO_2	0.75V/SiTi(30)
1.5%V_2O_5/SiO_2	1.5V/Si
1.5%V_2O_5/TiO_2	1.5V/Ti
1.5%V_2O_5/SiO_2 + 30%TiO_2	1.5V/SiTi(30)
2.5%V_2O_5/SiO_2 + 30%TiO_2	2.5V/SiTi(30)

3.1. Characterization of Materials

The catalytic materials prepared for this study were characterized using different analytical techniques. The **BET-BJH** (Brunauer-Emmett–Teller Barret-Joyner-Halenda) method was used to determine the specific surface areas, pore volumes, and pore sizes of all the prepared materials. Nitrogen adsorption–desorption isotherms were recorded at −196 °C using an ASAP 2020 Micrometrics apparatus (Norcross, GA, USA). Before N_2 adsorption, the samples were degassed at 300 °C and kept under vacuum for 2 h.

X-ray fluorescence analyses **(XRF**) were carried out to study the V, Si, and Ti amounts on the catalyst samples. 0.2 g of the studied sample was mixed with 8.5 g of flux in a Pt-Au crucible followed by melting in an Eagon 2 furnace at 1150 °C. The analysis was performed with an Axios mAX X-ray fluorescence spectrometer (PANalytical, Almelo, The Netherlands).

X-ray diffractometer **(XRD)** Siemens D5000 was used to characterize the crystalline structure of the catalyst materials. Analysis data was recorded between 10° and 80°, with a step of 0.040°. The crystallite size of the active phase and support was estimated using the Scherrer formula:

$$D = \frac{k\lambda}{\beta_c \times \cos\theta}$$

where k is the shape factor ($k = 0.94$), λ is the wavelength of X-ray, θ is the Bragg angle, and β_c is the corrected line broadening defined as FWHM (full width at half maximum).

X-ray photoelectron spectroscopy **(XPS)** analysis was carried out by a Thermo Fischer Scientific ESCALAB 250Xi instrument (Waltham, MA, USA) using Al Kα (1486.6 eV) radiation to excite photoelectrons. The binding energy was normalized with respect to the position of the C1s peak at 284.8 eV. The XPS analysis was performed on 3 fresh catalyst samples: 1.5%V/Si, 1.5%V/Ti and 1.5%V/SiTi(30). The samples were put on an indium substrate and placed inside a vacuum chamber. Thermo Avantage software (v5.957, Thermo Fisher Scientific Inc., Waltham, MA, USA) was used in data analysis. Smart background subtraction was used and the spectra of O 1s, C 1s, Si 2p, Ti 2p and V 2p were recorded.

Temperature-programmed desorption measurements of ammonia (**NH_3-TPD**) were carried out by AutoChem II 2920 equipment (Micromeritics Instrument Corp., Norcross, GA, USA). A powder-form catalyst sample was placed inside the reactor and pretreated in a Helium flow (50 cm^3 min^{-1}) from room temperature to 500 °C at the rate of 5 °C min^{-1} for 30 min. The sample was then cooled to room temperature (He 50 cm^3 min^{-1}). The adsorption of 15% NH_3 in He (50 cm^3 min^{-1}) was carried out at RT for 60 min, and then the sample was flushed with He for 30 min to remove any physisorbed ammonia. TPD was performed in a He flow by raising the temperature to 550 °C with a rate of 5 °C min^{-1}. Sample amount of 100 mg was used for Si-containing catalysts and 180 mg for pure Ti due to significantly lower surface area. The desorbed amount of NH_3 was analyzed by a TCD detector. The area between 40 °C and 500 °C was used for determination of the total acidity of the samples.

Scanning transmission electron microscope (**STEM**) studies were carried out to analyze the particle size and the distribution of the vanadium pentoxide on the surface of the supports. The measurements were done using a JEOL JEM-2200FS apparatus (JEOL Ltd., Tokyo, Japan). The acceleration voltage of 200 kV was used. For the measurements, the catalyst samples were dispersed on a copper grid with ethanol. The apparatus was equipped with an Energy-Dispersive X-ray Spectrometer (EDS) apparatus (JEOL Dry SD100GV). The EDS was used to identify the absorbed chemical elements on the fresh catalysts. The measured catalysts were fresh 1.5V/Si, 1.5V/Ti and 1.5V/SiTi(30).

The **Raman** spectra were collected with a Timegate® Raman Spectrometer (Oulu, Finland) with a pulsed 532 nm fiber coupled laser and a rapid SPAD-detector. The data were collected with a Raman shift range from 150 to 1150 cm^{-1}. Data was curve fitted and analyzed with a Shsqui Matlab based software (v0.981, Timegate Instruments Oy, Oulu, Finland). The fresh 1.5V/Si, 1.5V/Ti and 1.5V/SiTi30 were measured and the measurement was repeated after the 8 h stability tests.

3.2. Catalytic Oxidation Tests

The catalytic partial oxidation tests were performed in a laboratory scale tubular quartz reactor. The experimental set-up presented in our previous work [21] was modified for further studies with a few basic improvements. The current set-up is presented in Figure 13. All the gas lines after the evaporator (heated to ~70 °C) were heated to 180 °C to avoid the condensation of the evaporated compound on the tube surfaces. Some condensation of methanol may still occur as the reactor part of the set-up is in the room temperature in the beginning of each test. Relatively high GHSV (~94,000 h^{-1}) was used in the experiments and the experimental procedure was following the same path as presented in the previous work [21].

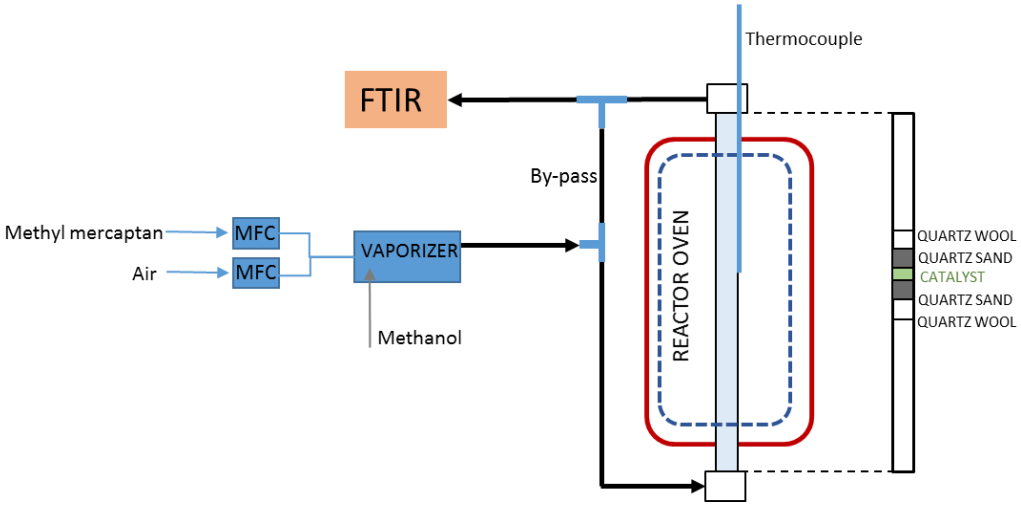

Figure 13. The experimental set-up for the catalyst activity testing.

All the experiments were conducted with 100 mg of a catalyst in the powder form. The feed concentration in each test was 500 ppm of methanol (Merck, Darmstadt, Germany) and 500 ppm of methyl mercaptan (Oy AGA Ab, Espoo, Finland) in a mixture. The reaction temperature was raised from room temperature to 500 °C with a heating rate of 5 °C min^{-1}. The outlet gas composition was analyzed by using a Gasmet FTIR Cr-2000 (Helsinki, Finland) analyzer equipped with an MCT detector. The following compounds were analyzed in each of the catalytic tests: carbon dioxide CO_2, carbon monoxide CO, nitrogen monoxide NO, nitrogen dioxide NO_2, nitrous oxide N_2O, sulfur dioxide SO_2, sulfur trioxide SO_3, methane CH_4, formaldehyde CH_2O, methyl mercaptan CH_4S, dimethyl sulfide C_2H_6S, dimethyl disulfide $C_2H_6S_2$, formic acid CH_2O_2, and methanol CH_4O. First the supports Si and Ti and mixed oxides SiTi(10), SiTi(30), and SiTi(60) were tested to find the possible changes in activity with respect to the Si:Ti ratio. The activity experiments were continued to study the effect of different vanadia loadings. The catalyst stability and repeatability of the catalytic tests were examined by testing the same catalyst in the same experimental conditions twice. The stabilities of 1.5 V catalysts were also tested in longer-term (8 h) experiments to gain some indication of the durability of the material. In 8 h tests, the catalyst amount of 200 mg was used. The same procedure as in the activity tests was used and the temperature was kept at the optimal formaldehyde production temperature (500 °C or lower) for 8 h.

4. Conclusions

V_2O_5 catalysts supported on SiO_2-TiO_2 have been characterized and tested in the oxidation of methanol and methyl mercaptan to formaldehyde. The results of the V_2O_5/SiO_2 + TiO_2 were compared with those obtained for V_2O_5/SiO_2 and V_2O_5/TiO_2 catalysts, showing that the composition of the support has a significant role in the catalytic behavior. The current oxidation results prove that silica–titania supported vanadia catalysts show good potential for use in the oxidation of sulfur contaminated methanol to formaldehyde. In the laboratory scale oxidation tests, significantly higher formaldehyde yields were achieved with the mixed silica–titania support. The important role of vanadium pentoxide in the catalyst is evident; the addition of the active compound results in higher activity of the catalysts, and lowers the optimal temperature of the reaction in which the desired partial oxidation products are formed. As expected, applying titania onto silica results in a higher surface area, which allows a good dispersion of vanadia. The acidity of the materials was dependent on the Si:Ti ratio of the support, but no solid conclusions about the role of the acidity in the activity of the catalysts in oxidation of methanol and methyl mercaptan could be made based on these findings. More detailed information on the surface of the catalysts and the reaction mechanisms is needed to

optimize these materials further. For example, the role of the quality of the acid sites as well as the effect of the vanadia dispersion should be detailed.

Acknowledgments: This work was carried out with the financial support of the Academy of Finland (ELECTRA-project), the Emil Aaltonen Foundation, the Walter Ahlström Foundation, and the Tauno Tönning foundation. The authors also gratefully acknowledge the No-Waste project funding from the European Union Seventh Framework Programme (FP7), Marie Curie Actions under grant agreement no. PIRSES-GA-2012-317714. Jorma Penttinen, Kaisu Ainassaari, Markus Riihimäki, and Zouhair El Assal are acknowledged for their valuable help with the characterization of catalysts and Kirsi Ahtinen for her help with practical laboratory work. The Center of Microscopy and Nanotechnology of the University of Oulu is also acknowledged.

Author Contributions: N.K. designed the work presented in this article, performed most of the laboratory tests, and performed the literature search and wrote the paper. T.L. took part in experimental parts of this paper. She performed some parts of the material characterizations and took part in analysis of the activity measurements. A.M. took part in the material preparation phase of the work. S.O. was the main advisor of the work and took part in each phase of the work. R.L.K. is the principal supervisor of the thesis work of N.K. and thus has the main responsibility in all actions related to the manuscript.

Conflicts of Interest: The authors declare no conflict of interest.

References

1. Itoh, M.; Hattori, H.; Tanabe, K. The acidic properties of TiO_2-SiO_2 and its catalytic activities for the amination of phenol, the hydration of ethylene and the isomerization of butene. *J. Catal.* **1974**, *35*, 225–231. [CrossRef]
2. Stakheev, A.Y.; Shpiro, E.S.; Apijok, J. XPS and XAES study of TiO_2-SiO_2 mixed oxide system. *J. Phys. Chem.* **1993**, *97*, 5668–5672. [CrossRef]
3. Topsoe, N.Y.; Topsoe, H.; Dumesic, J.A. Vanadia/Titania Catalysts for Selective Catalytic Reduction (SCR) of Nitric-Oxide by Ammonia. *J. Catal.* **1995**, *151*, 226–240. [CrossRef]
4. Klein, S.; Thorimbert, S.; Maier, W.F. Amorphous Microporous Titania–Silica Mixed Oxides: Preparation, Characterization, and Catalytic Redox Properties. *J. Catal.* **1996**, *163*, 476–488. [CrossRef]
5. Walters, J.K.; Rigden, J.S.; Dirken, P.J.; Smith, M.E.; Howells, W.S.; Newport, R.J. An atomic-scale study of the role of titanium in TiO_2:SiO_2 sol–gel materials. *Chem. Phys. Lett.* **1997**, *264*, 539–544. [CrossRef]
6. Watson, R.B.; Ozkan, U.S. K/Mo Catalysts Supported over Sol–Gel Silica–Titania Mixed Oxides in the Oxidative Dehydrogenation of Propane. *J. Catal.* **2000**, *191*, 12–29. [CrossRef]
7. Kobayashi, M.; Kuma, R.; Masaki, S.; Sugishima, N. TiO_2-SiO_2 and V_2O_5/TiO_2-SiO_2 catalyst: Physico-chemical characteristics and catalytic behavior in selective catalytic reduction of NO by NH_3. *Appl. Catal. B Environ.* **2005**, *60*, 173–179. [CrossRef]
8. Morosanova, E.I. Silica and silica–titania sol–gel materials: Synthesis and analytical application. *Talanta* **2012**, *102*, 114–122. [CrossRef] [PubMed]
9. Nizar, U.K.; Efendi, J.; Yuliati, L.; Gustiono, D.; Nur, H. A new way to control the coordination of titanium (IV) in the sol–gel synthesis of broom fibers-like mesoporous alkyl silica–titania catalyst through addition of water. *Chem. Eng. J.* **2013**, *222*, 23–31. [CrossRef]
10. Jehng, J.M.; Wachs, I.E. The molecular structures and reactivity of V_2O_5/TiO_2/SiO_2 catalysts. *Catal. Lett.* **1992**, *13*, 9–19. [CrossRef]
11. Galán-Fereres, M.; Mariscal, R.; Alemany, L.J.; Fierro, J.L.G.; Anderson, J.A. Ternary V–Ti–Si catalysts and their behaviour in the CO + NO reaction. *J. Chem. Soc. Faraday Trans.* **1994**, *90*, 3711–3718. [CrossRef]
12. Quaranta, N.E.; Soria, J.; Cortés Corberán, V.; Fierro, J.L.G. Selective Oxidation of Ethanol to Acetaldehyde on V_2O_5/TiO_2/SiO_2 Catalysts. *J. Catal.* **1997**, *171*, 1–13. [CrossRef]
13. Reiche, M.A.; Ortelli, E.; Baiker, A. Vanadia grafted on TiO_2–SiO_2, TiO_2 and SiO_2 aerogels Structural properties and catalytic behaviour in selective reduction of NO by NH_3. *Appl. Catal. B Environ.* **1999**, *23*, 187–203. [CrossRef]
14. Gao, X.; Bare, S.R.; Fierro, J.L.G.; Wachs, I.E. Structural Characteristics and Reactivity/Reducibility Properties of Dispersed and Bilayered V_2O_5/TiO_2/SiO_2 Catalysts. *J. Phys. Chem. B* **1999**, *103*, 618–629. [CrossRef]
15. Burcham, L.J.; Deo, G.; Gao, X.; Wachs, I.E. In situ IR, Raman, and UV-Vis DRS spectroscopy of supported vanadium oxide catalysts during methanol oxidation. *Top. Catal.* **2000**, *11–12*, 85–100. [CrossRef]

16. Monaci, R.; Rombi, E.; Solinas, V.; Sorrentino, A.; Santacesaria, E.; Colon, G. Oxidative dehydrogenation of propane over $V_2O_5/TiO_2/SiO_2$ catalysts obtained by grafting titanium and vanadium alkoxides on silica. *Appl. Catal. A Gen.* **2001**, *214*, 203–212. [CrossRef]
17. Dias, C.R.; Portela, M.F.; Bañares, M.A.; Galán-Fereres, M.; López-Granados, M.; Peña, M.A.; Fierro, J.L.G. Selective oxidation of o-xylene over ternary V-Ti-Si catalysts. *Appl. Catal. A Gen.* **2002**, *224*, 141–151. [CrossRef]
18. Keränen, J.; Guimon, C.; Iiskola, E.; Auroux, A.; Niinistö, L. Atomic layer deposition and surface characterization of highly dispersed titania/silica-supported vanadia catalysts. *Catal. Today* **2003**, *78*, 149–157. [CrossRef]
19. Burgess, T.L.; Gibson, A.G.; Furstein, S.J.; Wachs, I.E. Converting waste gases from pulp mills into value-added chemicals. *Environ. Prog.* **2002**, *21*, 137–141. [CrossRef]
20. Wachs, I.E. Treating Methanol-Containing Waste Gas Streams. U.S. Patent 5907066, 6 March 2001.
21. Koivikko, N.; Laitinen, T.; Ojala, S.; Pitkäaho, S.; Kucherov, A.; Keiski, R.L. Formaldehyde production from methanol and methyl mercaptan over titania and vanadia based catalysts. *Appl. Catal. B Environ.* **2011**, *103*, 72–78. [CrossRef]
22. Wang, Q.; Madix, R.J. Partial oxidation of methanol to formaldehyde on a model supported monolayer vanadia catalyst: Vanadia on TiO_2(1 1 0). *Surf. Sci.* **2002**, *496*, 51–63. [CrossRef]
23. Goodrow, A.; Bell, A.T. A theoretical investigation of the selective oxidation of methanol to formaldehyde on isolated vanadate species supported on titania. *J. Phys. Chem. C* **2008**, *112*, 13204–13214. [CrossRef]
24. Bronkema, J.L.; Bell, A.T. Mechanistic Studies of Methanol Oxidation to Formaldehyde on Isolated Vanadate Sites Supported on MCM-48 Mechanistic Studies of Methanol Oxidation to Formaldehyde on Isolated Vanadate Sites Supported on MCM-48. *J. Phys. Chem. C* **2007**, *111*, 420–430. [CrossRef]
25. Bronkema, J.L.; Bell, A.T. Mechanistic studies of methanol oxidation to formaldehyde on isolated vanadate sites supported on high surface area zirconia. *J. Phys. Chem. C* **2008**, *112*, 6404–6412. [CrossRef]
26. Vining, W.C.; Strunk, J.; Bell, A.T. Investigation of the structure and activity of $VOx/ZrO_2/SiO_2$ catalysts for methanol oxidation to formaldehyde. *J. Catal.* **2011**, *281*, 222–230. [CrossRef]
27. Burcham, L.J.; Wachs, I.E. The origin of the support effect in supported metal oxide catalysts: In situ infrared and kinetic studies during methanol oxidation. *Catal. Today* **1999**, *49*, 467–484. [CrossRef]
28. Kropp, T.; Paier, J.; Sauer, J. Oxidative dehydrogenation of methanol at ceria-supported vanadia oligomers. *J. Catal.* **2017**, *352*, 382–387. [CrossRef]
29. Kim, M.H.; Ebner, J.R.; Friedman, R.M.; Vannice, M.A. Determination of Metal Dispersion and Surface Composition in Supported Cu–Pt Catalysts. *J. Catal.* **2002**, *208*, 381–392. [CrossRef]
30. Wachs, I.E. Catalysis science of supported vanadium oxide catalysts. *Dalt. Trans.* **2013**, *42*, 11762–11769. [CrossRef] [PubMed]
31. Chary, K.V.R.; Kishan, G.; Lakshmi, K.S.; Ramesh, K. Studies on dispersion and reactivity of vanadium oxide catalysts supported on titania. *Langmuir* **2000**, *16*, 7192–7199. [CrossRef]
32. Mendialdua, J.; Casanova, R.; Barbaux, Y. XPS studies of V_2O_5, V_6O_{13}, VO_2 and V_2O_3. *J. Electron Spectrosc. Relat. Phenom.* **1995**, *71*, 249–261. [CrossRef]
33. Silversmit, G.; Depla, D.; Poelman, H.; Marin, G.B.; De Gryse, R. Determination of the V2p XPS binding energies for different vanadium oxidation states (V^{5+} to V^{0+}). *J. Electron Spectrosc. Relat. Phenom.* **2004**, *135*, 167–175. [CrossRef]
34. Biesinger, M.C.; Payne, B.P.; Grosvenor, A.P.; Lau, L.W.M.; Gerson, A.R.; Smart, R.S.C. Resolving surface chemical states in XPS analysis of first row transition metals, oxides and hydroxides: Cr, Mn, Fe, Co and Ni. *Appl. Surf. Sci.* **2011**, *257*, 2717–2730. [CrossRef]
35. Demeter, M.; Neumann, M.; Reichelt, W. Mixed-valence vanadium oxides studied by XPS. *Surf. Sci.* **2000**, *454*, 41–44. [CrossRef]
36. Odriozola, J.A.; Soria, J.; Somorjai, G.A.; Heinemann, H.; de la Garcia Banda, J.F.; Lopez Granados, M.; Conesa, J.C. Adsorption of nitric oxide and ammonia on vanadia-titania catalysts: ESR and XPS studies of adsorption. *J. Phys. Chem.* **1991**, *95*, 240–246. [CrossRef]
37. Gao, X.; Bare, S.R.; Fierro, J.L.G.; Banares, M.A.; Wachs, I.E. Preparation and in-situ Spectroscopic Characterization of Molecularly Dispersed Titanium Oxide on Silica. *J. Phys. Chem. B* **1998**, *102*, 5653–5666. [CrossRef]

38. Gao, X.; Bare, S.R.; Weckhuysen, B.M.; Wachs, I.E. In Situ Spectroscopic Investigation of Molecular Structures of Highly Dispersed Vanadium Oxide on Silica under Various Conditions. *J. Phys. Chem. B* **1998**, *102*, 10842–10852. [CrossRef]
39. Deo, G.; Wachs, I.E. Predicting molecular structures of surface metal oxide species on oxide supports under ambient conditions. *J. Phys. Chem.* **1991**, *95*, 5889–5895. [CrossRef]
40. Blasco, T.; Nieto, J.M.L. Oxidative dyhydrogenation of short chain alkanes on supported vanadium oxide catalysts. *Appl. Catal. A Gen.* **1997**, *157*, 117–142. [CrossRef]
41. Rumble, J.R. (Ed.) *CRC Handbook of Chemistry and Physics*, 98th ed.; Internet Version 2018; CRC Press: Boca Raton, FL, USA, 2017.
42. Laitinen, T.; Ojala, S.; Koivikko, N.; Mouammine, A.; Keiski, R.L. Stability of a vanadium-based catalyst in the partial oxidation of a mixture of methanol and methyl mercaptan. In Proceedings of the 17th Nordic Symposium on Catalysis, Lund, Sweden, 14–16 June 2016.
43. Tanabe, K.; Sumiyoshi, T.; Shibata, K.; Kiyoura, T.; Kitagawa, J. A new hypothesis regarding the surface acidity of binary metal oxides. *Bull. Chem. Soc. Jpn.* **1974**, *47*, 1064–1066. [CrossRef]
44. Keränen, J.; Carniti, P.; Gervasini, A.; Iiskola, E.; Auroux, A.; Niinistö, L. Preparation by atomic layer deposition and characterization of active sites in nanodispersed vanadia/titania/silica catalysts. *Catal. Today* **2004**, *91–92*, 67–71. [CrossRef]
45. Mouammine, A.; Ojala, S.; Pirault-Roy, L.; Bensitel, M.; Keiski, R.; Brahmi, R. Catalytic partial oxidation of methanol and methyl mercaptan: Studies on the selectivity of TiO_2 and CeO_2 supported V_2O_5 catalysts. *Top. Catal.* **2013**, *56*, 650–657. [CrossRef]
46. Went, G.T.; Oyama, S.T.; Bell, A.T. Laser Raman spectroscopy of supported vanadium oxide catalysts. *J. Phys. Chem.* **1990**, *94*, 4240–4246. [CrossRef]
47. Vuurman, M.A.; Wachs, I.E.; Hirt, A.M. Structural determination of supported vanadium pentoxide-tungsten trioxide-titania catalysts by in situ Raman spectroscopy and X-ray photoelectron spectroscopy. *J. Phys. Chem.* **1991**, *95*, 9928–9937. [CrossRef]
48. Wachs, I.E.; Deo, G.; Weckhuysen, B.M.; Andreini, A.; Vuurman, M.A.; de Boer, M.; Amiridis, M.D. Selective Catalytic Reduction of NO with NH_3 over Supported Vanadia Catalysts. *J. Catal.* **1996**, *161*, 211–221. [CrossRef]
49. Reuss, G.; Disteldorf, W.; Gamer, A.O.; Hilt, A. Formaldehyde. In *Ulmann's Encyclopedia of Industrial Chemistry*; Wiley-VCH: Weinheim, Germany, 2012; Volume 15, pp. 735–768.